- The mid-depth Southern Ocean (~500–1500 m) continued to warm at rates up to 0.02°C yr$^{-1}$ while the surface ocean continued to cool by −0.015° to −0.05°C yr$^{-1}$, freshen, and acidify.

The state of Antarctica's climate, weather, ice, ocean, and ozone in 2017 are presented below. Place names used throughout this chapter are provided in Fig. 6.1.

*b. Atmospheric circulation and surface observations*—K. R. Clem, S. Barreira, R. L. Fogt, S. Colwell, C. Costanza, L. M. Keller, and M. A. Lazzara.

Atmospheric circulation patterns are the main drivers of all other aspects of this climate summary, affecting sea ice, precipitation, weather records, and even ozone loss. Moreover, long-term changes in climate are impacting ocean circulation (e.g., Schneider et al. 2012) and surface melt patterns (e.g., van den Broeke 2005) and thereby affecting the ice mass balance of the Antarctic ice sheet.

For this detailed analysis of the atmospheric circulation and temperature and pressure anomalies, the European Centre for Medium-Range Weather Forecasts interim reanalysis (ERA-Interim) is utilized as it is shown to be the most reliable representation of Antarctic tropospheric pressure and temperature among all modern global reanalyses (Bracegirdle and Marshall 2012). Figure 6.2 shows the monthly geopotential height (Fig. 6.2a) and temperature (Fig. 6.2b) anomalies averaged over the polar cap (60°–90°S) and the monthly circumpolar zonal wind (Fig. 6.2c) anomalies averaged over 50°–70°S. Anomalies are contoured and the standard deviation level is indicated by colored shading. The year was grouped into four periods characterized by relatively consistent climatic fea-

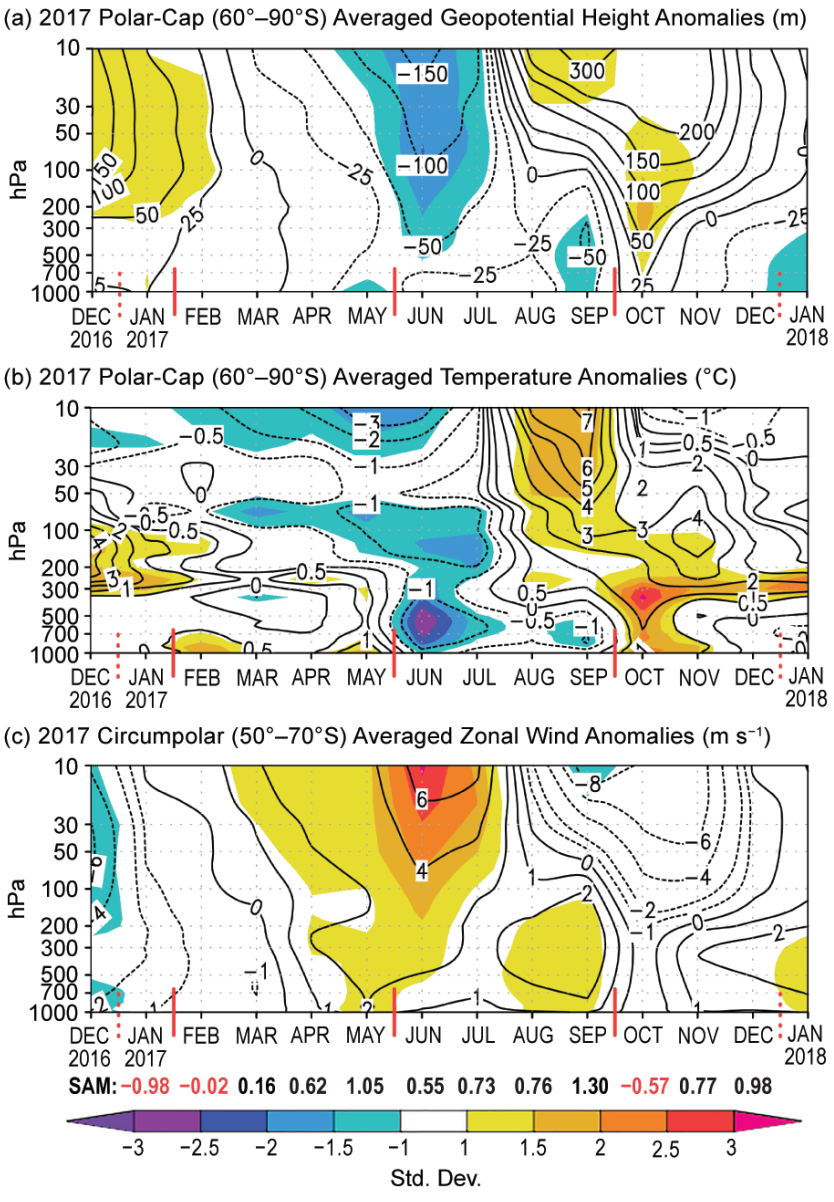


**Fig. 6.2. Area-averaged (weighted by cosine of latitude) monthly anomalies over the southern polar region in 2017 relative to 1981–2010: (a) polar cap (60°–90°S) averaged geopotential height anomalies (contour interval is 50 m up to ±200 m with additional contour at ±25 m, and 100 m contour interval after ±200 m); (b) polar cap averaged temperature anomalies (contour interval is 1°C with additional contour at ±0.5°C); (c) circumpolar (50°–70°S) averaged zonal wind anomalies (contour interval is 2 m s$^{-1}$ with additional contour at ±1 m s$^{-1}$). Shading depicts std. dev. of monthly anomalies from the 1981–2010 climatological average as indicated by color bar at bottom. (Source: ERA-Interim reanalysis.) Red vertical bars indicate the four climate periods used for compositing in Fig. 6.3; the dashed lines near Dec 2016 and Dec 2017 indicate circulation anomalies wrapping around the calendar year. Values from the NOAA CPC Antarctic Oscillation index (herein referred to as the SAM index) are shown below (c) in black (positive values) and red (negative values).**

tures: January, February–May, June–September, and October–December. These periods are indicated by vertical red bars at the bottom of each panel in Fig. 6.2. Anomalies for the four groups from their respective group climatological mean are shown in Fig. 6.3, with surface pressure anomalies shown on the left and 2-m temperature anomalies shown on the right. Monthly temperature and pressure anomalies during 2017 are also displayed in Fig. 6.4 for three staffed stations (Amundsen–Scott, Casey, and Rothera) and three automatic weather stations (AWS; Byrd, Dome C II, and Ferrell) to examine the monthly variability and extreme events for the surface conditions across the continent.

January 2017 was distinct from the rest of the year with positive pressure anomalies over the continent and primarily negative pressure anomalies between 40° and 60°S (Fig. 6.3a) and slightly weaker-than-average circumpolar westerlies throughout the troposphere and lower stratosphere (Fig. 6.2c). The January circulation pattern is consistent with the negative phase of the southern annular mode (SAM) which continued from late 2016 [the SAM index from NOAA's Climate Prediction Center (CPC) in January was −0.98], and it marks the transition of the late 2016 circulation to opposite sign anomalies in autumn 2017. At the surface, a strong high pressure anomaly was present over the South Pacific poleward to the Amundsen Sea, which through altered temperature advection and sea ice conditions produced negative temperature anomalies of ~1°C across the Antarctic Peninsula (Figs. 6.3a,b). These features weakened after January, and from February through May they were replaced by an anomalously deep Amundsen Sea Low centered over the northwest Amundsen Sea into the South Pacific (Fig. 6.3c; 6–9 hPa and 2–3 standard deviations below average). The anomalous cyclonic circulation, in conjunction with an anticyclone anomaly in the northwest Weddell Sea, produced well-above-average temperatures across much of West Antarctica during late summer and autumn spanning the western Antarctic Peninsula, Amundsen Sea Embayment, Marie Byrd Land, and Ross Ice Shelf (Fig. 6.3d; 2°–5°C and >3 standard deviations above average). Temperatures at the Byrd AWS in central West Antarctica were 2°–5°C above average during February–May, and record maximum monthly mean temperatures were observed on the Antarctic Peninsula in March at both Marambio (−2°C) and Rothera (1.2°C; Fig. 6.4c); Dome C II AWS, on the East Antarctic plateau, reported record low monthly mean temperatures in March (−57.1°C, Fig. 6.4e), nearly 5°C below average.

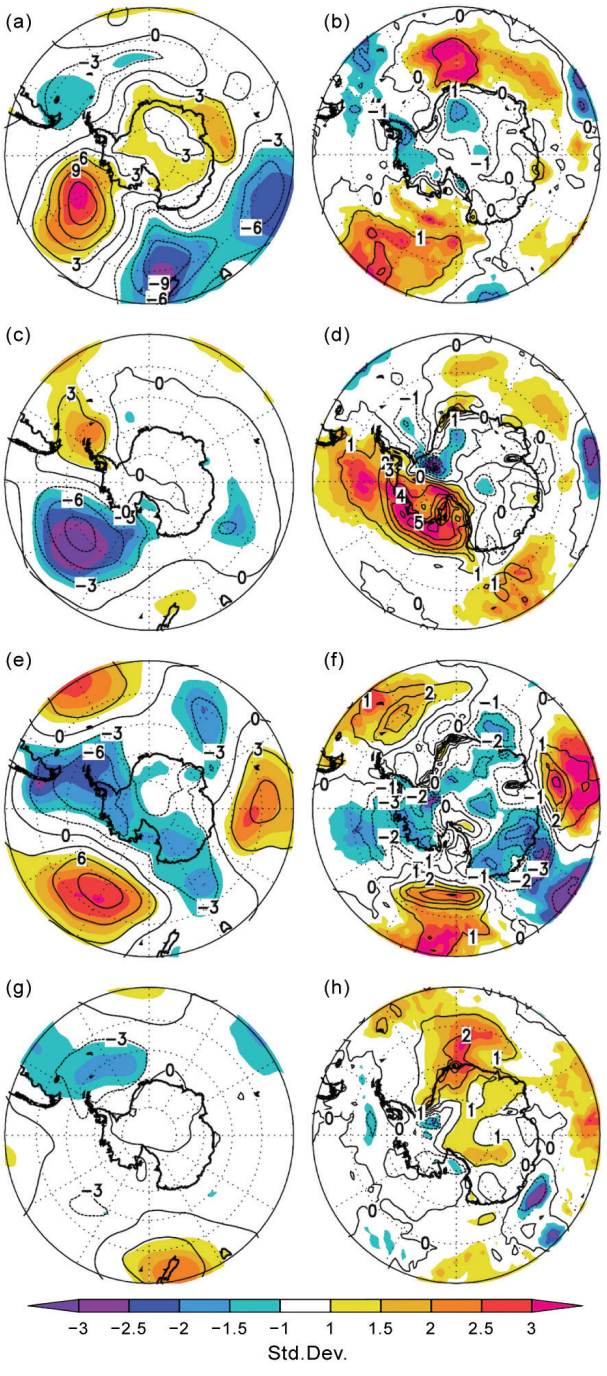


**Fig. 6.3. (left) Surface pressure anomalies and (right) 2-m temperature anomalies relative to each group's 1981–2010 climatological average for (a) and (b) Jan 2017; (c) and (d) Feb–May 2017; (e) and (f) Jun–Sep 2017; and (g) and (h) Oct–Dec 2017. Contour interval for surface pressure anomalies is 3 hPa and 1°C for 2-m temperature anomalies. Shading depicts std. dev. of anomalies relative to the 1981–2010 average of each group. (Source: ERA-Interim reanalysis.)**

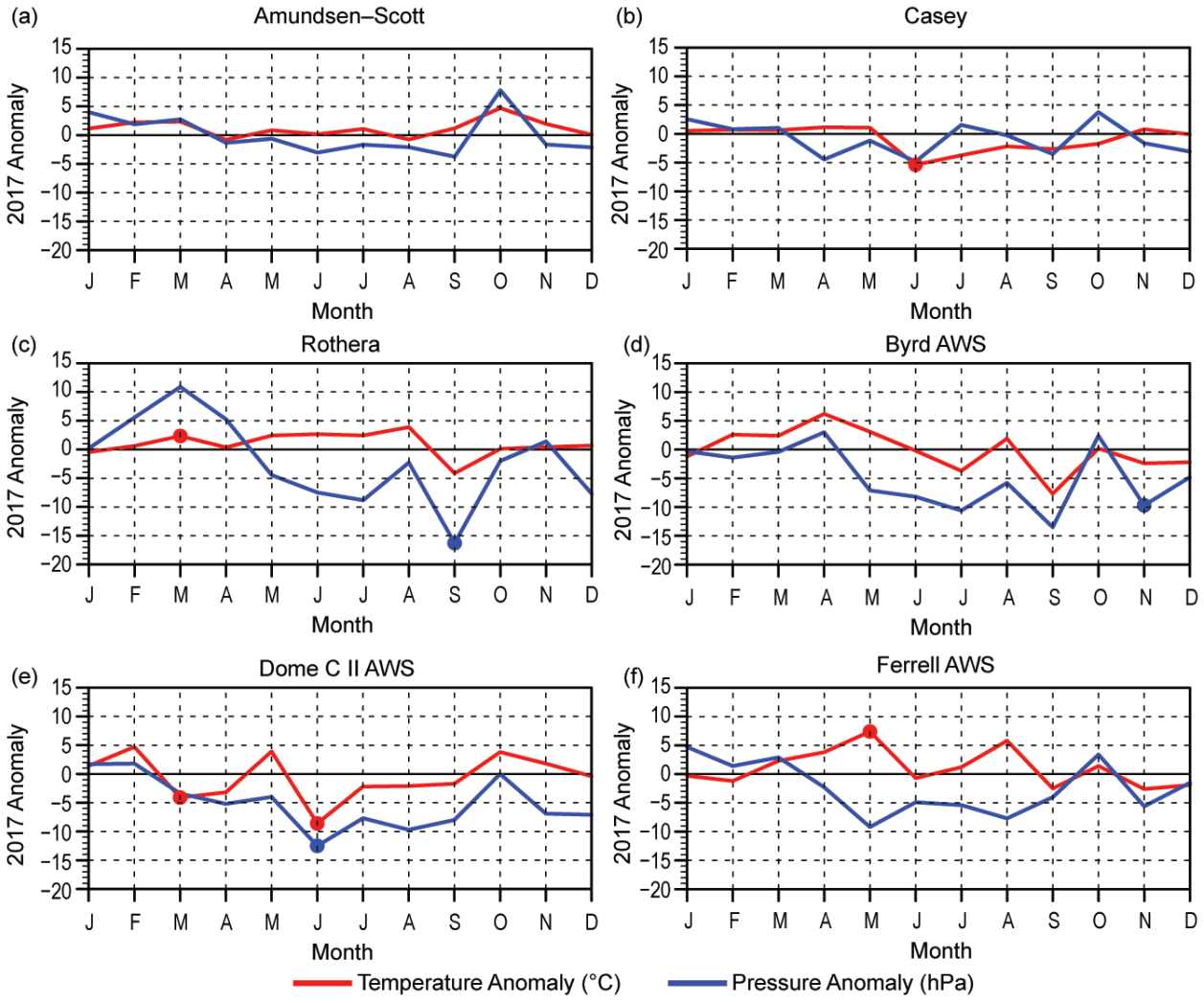


**Fig. 6.4. Monthly Antarctic climate anomalies during 2017 at six representative stations [three staffed (a)–(c), and three automatic (d)–(f)]. Anomalies for temperature (°C) are shown in red and MSLP/surface pressure (hPa) in blue are shown, with filled circles denoting record anomalies for a given month at each station in 2017. All anomalies are based on differences from the monthly 1981–2010 averages. Observational data start in 1957 for Amundsen–Scott, 1959 for Casey, 1976 for Rothera, 1980 for Byrd AWS, and 1981 Dome C II and Ferrell AWS.**

During April (not shown), negative pressure anomalies developed over Wilkes Land and Queen Maud Land, and the associated northerly flow was an important contributor to the late advance of sea ice in the western Ross and eastern Weddell Seas; these cyclonic circulation anomalies were part of a larger shift in the Antarctic circulation as captured to some extent in the polar-cap-averaged geopotential height (Fig. 6.2a) and circumpolar zonal wind anomalies (Fig. 6.2c), both of which changed sign in April and intensified in May. At Casey Station, located in Wilkes Land in coastal East Antarctica, pressure anomalies were the lowest in April, consistent with this circulation shift. On the eastern side of this low pressure system, the northerly flow increased temperatures across the Ross Ice Shelf, and Ferrell AWS reported a record monthly mean maximum temperature for May of –23.1°C, 7.4°C warmer than the climatological average (Fig. 6.4f).

During the winter months (June–September), a pronounced zonal wave-three pattern developed, characterized by three anomalous ridges along 50°S centered at 90°E, 150°W, and 30°W and a deep low pressure anomaly over the Antarctic Peninsula (Fig. 6.3e). Temperatures were generally below average across the continent, especially on the eastern side of the midlatitude ridges/western side of the troughs, where southerly flow produced cool conditions. Colder-than-average winter temperatures were also observed throughout the troposphere and

stratosphere, accompanied by negative geopotential height anomalies and stronger-than-average circumpolar westerlies in winter (Fig. 6.2); the stratospheric vortex exhibited the greatest positive anomalies of 4–6 m $s^{-1}$ above average during June. East Antarctica experienced its most negative temperature anomalies during 2017 in June (2°–6°C below average), with Casey (Fig. 6.4b) and Dome C II AWS (Fig. 6.4e) both setting record low monthly mean temperatures in June (−19.4°C and −57.1°C, respectively). West Antarctica saw its strongest cold anomalies during July (2°–4°C below average) and September (4°–8°C below average; see Byrd AWS temperature anomalies in Fig. 6.4d). The colder-than-average temperatures in September were partially due to the low pressure anomaly over the Antarctic Peninsula, reflected in the record negative monthly mean pressure of 971.3 hPa at Rothera (Fig 6.4c), more than 16 hPa below the climatological average.

A positive temperature/geopotential height anomaly developed in the stratosphere during September and propagated downward into the lower troposphere during October (Fig. 6.2). Positive pressure and temperature anomalies developed at the surface across much of the continent in October, reflected in the observations at Amundsen Scott in Fig. 6.4a; the strongest positive surface air temperature anomalies during October (not shown) were over interior portions of East Antarctica along the Transantarctic Mountains reaching 2°–4°C (> 3 standard deviations) above average, and Vostok Station in the central East Antarctic plateau set a record high monthly mean temperature in October of −51.1°C, 1.7°C higher than the previous record set in 2015. Averaged over the October–December period (Figs. 6.3g,h), the strongest positive temperature anomalies were over Queen Maud Land, while the rest of the continent experienced near-average to slightly-above-average temperatures and near-average pressure to close out 2017; exceptions include the Ross Ice Shelf where below-average temperatures were observed during November due to enhanced southerly flow from the development of an anomalous cyclone in the South Pacific that was consistent with the late austral spring La Niña conditions (see Section 4b) and a record monthly mean low surface pressure value at the Byrd AWS in November (787.7 hPa).

There were several record high monthly-mean wind speeds recorded at various AWS during the year. Ferrell had record high wind speeds in May (9.7 m $s^{-1}$), July (9.5 m $s^{-1}$), and August (10.6 m $s^{-1}$) and Marble Point had a record high wind speed in March (5.7 m $s^{-1}$). Byrd had a record high wind speed in May (10.6 m $s^{-1}$), and Dome C II had a record in October (5.4 m $s^{-1}$). Relay Station tied its record low wind speed in November (5.5 m $s^{-1}$). The record high wind speeds reflect the incidence of lower than normal pressure for much of the year (Figs. 6.3, 6.4).

*c. Net precipitation (P−E)*—D. H. Bromwich and S.-H. Wang

Precipitation minus evaporation/sublimation ($P-E$) closely approximates the surface mass balance over Antarctica (e.g., Bromwich et al. 2011; Lenaerts and van den Broeke 2012), except for near-coastal areas where wind-driven transport of snow and meltwater runoff can become significant factors. Precipitation variability is the dominant term for $P-E$ changes at regional and larger scales over the Antarctic continent. Precipitation and evaporation fields from the Japanese 55-year reanalysis (JRA-55; Kobayashi et al. 2015) were examined to assess Antarctic net precipitation ($P-E$) behavior for 2017. JRA-55, the second generation of JRA, has incorporated many improvements compared to its predecessor JRA-25 (Onogi et al. 2007; Bromwich et al. 2007). The JRA-55 is used here because of these improvements and its low latency, rather than ERA-Interim used elsewhere. Because of the highly uneven distribution of $P-E$ characteristics (from large Peninsula and coastal West Antarctica values >1000 mm $yr^{-1}$ to very low values <50 mm $yr^{-1}$ in the high interior), only annual $P-E$ changes are shown in Fig. 6.5.

Figure 6.5 shows the JRA-55 2017 and 2016 annual anomalies of $P-E$ (Figs. 6.5a,b) and mean sea level pressure (MSLP; Figs. 6.5c,d) departures from the 1981–2010 average. In general, annual $P-E$ anomalies over the high interior of the continent were small (within ±50 mm $yr^{-1}$), and larger anomalies were observed along the coast, consistent with the low and high net precipitation accumulation in these regions. From JRA-55, the 2016 positive anomalies located along the coast between Queen Maud Land and Mac Robertson Land (between 5°W and 60°E) became weak negative anomalies in 2017, most pronounced near 60°E. The weak negative anomalies over the American Highland (between 70° and 90°E) in 2016 became strongly positive in 2017. Both Queen Mary Land and Wilkes Land (between 90° and 125°E) remained strongly negative. The strong positive anomalies over Adélie Land and Victoria Land (between 125° and 175°E) became near-zero in 2017. The positive anomaly over the eastern Ross Ice Shelf in 2016 evolved into a larger positive anomaly that extended into interior Antarctica in 2017. The largest positive anomalies that were located over the Bellingshausen Sea and the southern Antarctic